Journal of MATERIALS RESEARCH

Article
DOI: 10.1557/jmr.2020.158

# Microstructure evolution and mechanical properties of the ZM61 alloy sheets under different pre-rolling and high strain rate rolling temperatures

Hongge Yan[1,2], Qin Wu[1,2,a)], Jihua Chen[1,2,b)], Weijun Xia[1,2], Min Song[3], Bin Su[1,2], Jiang Wu[1,2]

[1]School of Materials Science and Engineering, Hunan University, Changsha 410082, PR China
[2]Hunan Provincial Key Laboratory of Spray Deposition Technology & Application, Hunan University, Changsha 410082, PR China
[3]State Key Laboratory of Powder Metallurgy, Central South University, Changsha 410083, PR China
[a)]Address all correspondence to these authors. e-mail: 15074991154@163.com
[b)]e-mail: jihuachen2005@163.com

Received: 20 February 2020; accepted: 2 June 2020

**The microstructure evolution, dynamic recrystallization (DRX) and precipitation of the ZM61 alloy sheets prepared with different rolling conditions were studied. The DRX grain sizes ($d_{DRX}$) at four high strain rate rolling (HSRR) temperatures (275–350 °C) are 1.9, 2.3, 2.6 and 3.1 μm, respectively, while the DRX volume fractions ($f_{VDRX}$) are 69, 73, 76 and 82%, respectively. 300 °C is selected as the optimal HSRR temperature. The $d_{DRX}$ and $f_{VDRX}$ of the alloys prepared by pre-rolling (PR) at 300 °C + HSRR are 1.0 μm and 91%, respectively. The PR treatment does not change the types of the precipitates but promotes the precipitation. The tensile strength (UTS) of 369 MPa and yield strength (YS) of 261 MPa can be achieved by HSRR at 300 °C, while a further increase in both UTS and YS can be obtained by PR treatment.**

## Introduction

Mg alloys have a broad application prospect in automobile manufacture, aerospace and other fields due to their high specific strength and low density [1]. However, their industrial applications are severely limited by the poor formability, the difficulties in the subsequent deep processing and the disadvantages in mechanical properties as compared with Al and steel [2]. Grain refinement and precipitation strengthening are two promising means to improve the comprehensive mechanical properties of wrought Mg alloys [3, 4].

The temperature is an important factor in the recrystallization process, as it is a typical thermal activation process [5]. Peng et al. [6] have found that the critical strain of dynamic recrystallization (DRX) in the Mg–6Zn–1Mn alloy increases with the decreasing compression temperature, indicating that the lower temperature is unfavorable to DRX. DRX becomes easier with the increasing compression temperature, while the coarser DRX grains are obtained. The ultra-fine-grained Mg alloy sheets with high strength and plasticity have been successfully prepared by high strain rate rolling (HSRR) in our previous work [7]. However, the initial thickness of Mg alloy sheets for HSRR is relatively thin, which is not conducive to the industrial production. Moreover, the DRX degree should be further improved. Zhu et al. [8] have revealed that twinning would replace the dislocation slip as the main deformation mechanism during HSRR at the strain rate of 9.1 $s^{-1}$, resulting in the significant grain refinement effect. Song et al. [9] have reported that twins formed in pre-deformation can bring about the improvement in grain refinement strengthening and texture strengthening, so as to increase the strength of Mg alloys. The ZM61 alloy sheet with the average grain size of 0.8 μm and the DRX degree of 99% has been prepared *via* the combination of pre-rolling (PR) and the subsequent HSRR by Jiang et al. [10].

In our previous investigation, the ZM61 alloy sheet prepared with 20% PR strain at 300 °C followed by 80% HSRR strain at 300 °C exhibits tensile strength (UTS) of 392 MPa and elongation (EL) of 16.8% [11]. In this paper, the Mg–6Zn–1Mn (ZM61) alloys are subjected to HSRR with and without PR treatment at different temperatures, and the influences of deformation temperatures on microstructure evolution, DRX and precipitation behavior are examined, so as to explore a suitable way to further improve the comprehensive mechanical properties of the alloy sheets on the basis of the thick plate.

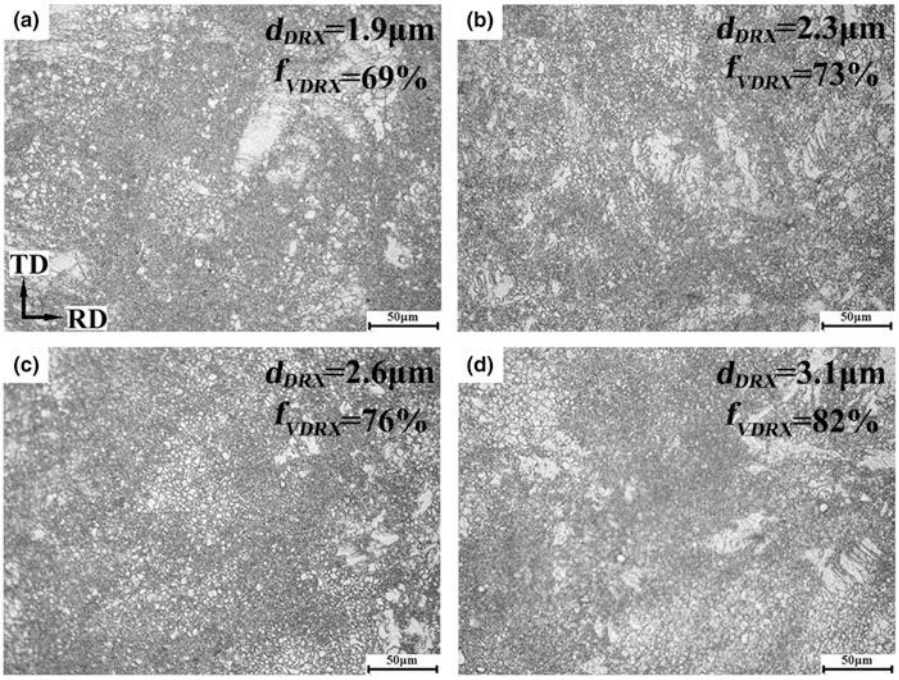


**Figure 1:** Optical images of the as-HSRRed ZM61 alloy prepared at different temperatures (a) 275 °C; (b) 300 °C; (c) 325 °C; (d) 350 °C.

The present study is beneficial to the theoretical research and the development of the as-HSRRed Mg alloy sheets.

## Result and Discussion

### As-HSRRed microstructures

Figure 1 shows the TD–RD microstructures of the as-HSRRed ZM61 alloy sheets rolled at different temperatures. A typical bimodal structure with fine equiaxed grains and coarse deformed structures can be found in the alloy rolled at 275 °C [Fig. 1(a)]. The grain size ($d_{DRX}$) and the volume fraction ($f_{VDRX}$) of DRX are 1.9 μm and 69%, respectively. When the rolling temperature increases to 300 °C [Fig. 1(b)], the $d_{DRX}$ increases to 2.3 μm and the $f_{VDRX}$ increases to 73%. The DRX degree and $d_{DRX}$ increase with the rolling temperature increasing to 325 °C [Fig. 1(c)]. The $d_{DRX}$ and $f_{VDRX}$ are 2.6 μm and 76%, respectively. However, some DRX grains grow up with the size about 7 μm with the rolling temperature of 350 °C [Fig. 1(d)], but the fine DRX grains are still dominant. The $d_{DRX}$ and $f_{VDRX}$ are 3.1 μm and 82%, respectively.

Table 1 shows the $d_{DRX}$ and $f_{VDRX}$ of the as-HSRRed ZM61 alloy sheets rolled at different rolling temperatures. It can be concluded that the $d_{DRX}$ and $f_{VDRX}$ increase with the higher rolling temperature during HSRR. The much lower DRX volume fraction and the poor structural homogeneity are obtained at 275 °C, while the grain growth occurs with the rolling temperature of 350 °C and higher, leading to the reduced fine-grained strengthening. Therefore, the optimal HSRR temperature in this experiment is 300 °C.

**TABLE 1:** Grain size and volume fraction of DRX under different deformation conditions.

| Deformation conditions | HSRR | | | | 300°CPR-20% +300° CHSRR-80% | 420°CPR-20% + 300 ° CHSRR-80% |
|---|---|---|---|---|---|---|
| | 275 °C | 300 °C | 325 °C | 350 °C | | |
| $d_{DRX}$/μm | 1.9 | 2.3 | 2.6 | 3.1 | 1.0 | 1.5 |
| $f_{VDRX}$/% | 69 | 73 | 76 | 82 | 91 | 93 |

### Microstructures of the alloys after HSRR with PR treatment

Figure 2 shows the microstructures of the alloy sheets prepared by PR, PR + annealing, PR + annealing + HSRR. As seen in Fig. 2(a), the high-density twin lamellae are obtained in the alloy experienced PR at 300 °C with the reduction of 20%. The coarse grains are divided into the smaller ones by twin lamellae and the twinning orientations differ in different grains. As shown in Fig. 2(b), the twin lamellae are still existent in the as-annealed alloys and the formation of some DRX grains is also observed. After HSRR at 300 °C [Fig. 2(c)], almost complete DRX regions featured with the small grain size are obtained and only a small number of un-DRXed regions are detected, indicating that PR promotes DRX and grain refinement. The $d_{DRX}$ and $f_{VDRX}$ are 1.0 μm and 91%, respectively. High density of twins and fine DRX grains are introduced after PR and annealing, and grain boundaries and twins are the preferential nucleation locations for DRX grains. The twins can induce the nucleation of secondary twins in the primary twins during the subsequent HSRR process and the

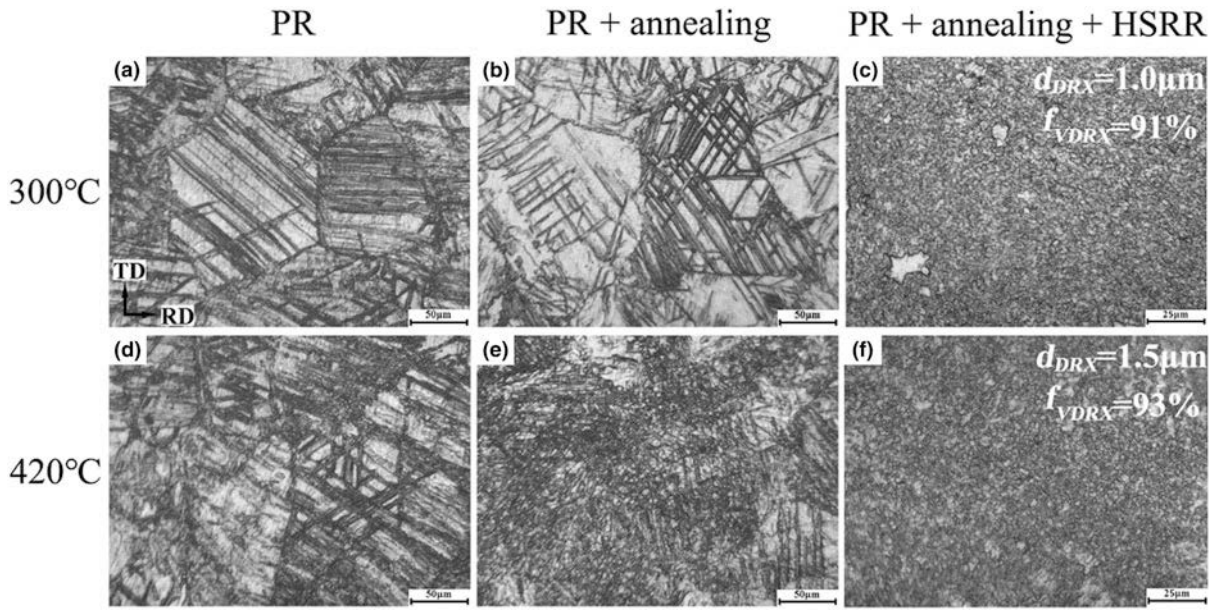


**Figure 2:** Optical images of the ZM61 alloys prepared by different processes.

hindering effect of the intersected twins on dislocation is greater than that of the single twin lamellar [12], which can promote the DRX process and refine the grains. Hong and Park et al. [13, 14] have found that the introduction of high density of twins, such as {10–12} tensile twins, in Mg alloys by PR can change the grain orientation and promote the DRX. In addition, pre-rolling can also induce the dynamic precipitation which leads to the precipitation strengthening, and the pinning effect of dynamic precipitates on the migration of DRX grain boundaries is also an effective mean to refine the grains [9].

Figures 2(d) and 2(e) show the microstructure of the alloy prepared by PR at 420 °C with a reduction of 20% and the corresponding as-annealed microstructure. It can be seen that the twin density in the annealed state is lower than the PR state at 300 °C and some DRX grains are found to form in the twin lamellae in the PR state at 420 °C [Fig. 2(d)]. After annealing [Fig. 2(e)], the twins and the original grain boundaries are almost replaced by the DRX grains. The $f_{VDRX}$ decreases, while the $d_{DRX}$ increases slightly after HSRR [Fig. 2(f)]. The $d_{DRX}$ and $f_{VDRX}$ are 1.5 μm and 93% for the alloy prepared by PR + annealing + HSRR, respectively. As shown in Table 1, the PR treatment can promote the DRX process, increase the $f_{VDRX}$ and refine the DRX grains. The $d_{DRX}$ and $f_{VDRX}$ increase with the higher PR temperature. It is worth noting that the $d_{DRX}$ of the alloy experienced PR at 300 °C is smaller than that experienced PR at 420 °C. As seen from Figs. 2(a) and 2(d), the initial microstructure changes from twins to the mixed structure composed of twins and DRX grains with the higher PR temperature. After annealing [Figs. 2(b) and 2(e)], the twins are existed in the alloy experienced PR at 300 °C, while the alloy experienced PR at 420 °C is composed of fine DRX grains. Therefore, the PR temperature has a certain influence on the DRX behavior in the subsequent HSRR process.

## Dynamic recrystallization behavior

Figure 3 shows the bright-field TEM images of the ZM61 alloys after HSRR with and without PR treatment. As shown in Figs. 3(a) and 3(b), a large number of fine DRX grains can be observed in the alloys as-HSRRed at 300 °C, with the grain size of about 2.3 μm. The existence of some twin lamellae can also be observed, as shown by the red arrow in Fig. 3(b), these twin lamellae can effectively coordinate the deformation and divide the original coarse grains into the smaller ones. At the same time, high-density dislocations in the twins can promote the nucleation of DRX grains. Zhu et al. [8] have reported that the twin-aided DRX mechanism is dominant in Mg alloys during HSRR. With PR at 300 °C [Fig. 3(c)], the DRX grain size decreases to about 1.0 μm and almost no twins are observed in the alloy. As shown in Fig. 3(d), the DRX grain size of the alloy prepared by PR at 420 °C + annealing + HSRR is 1.5 μm, which is still smaller than that of the alloy without PR. The twins and fine grains introduced by PR provide more nucleation sites for DRX during HSRR, which increases the nucleation rate and the DRX volume fraction and thus refines the grain size.

## Dynamic precipitation

For the Mg–Zn alloys, the maximum solid solubility of Zn in Mg is 6.2% [15], and the Zn content in the Mg–6Zn–1Mn

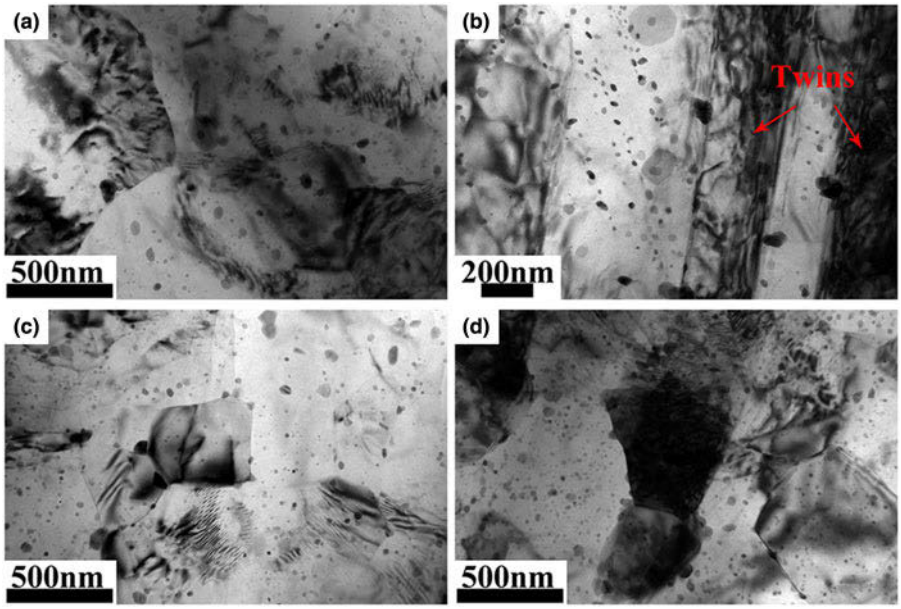


**Figure 3:** Bright-field TEM images of the alloy after HSRR with and without PR (a), (b) without PR, (c) with PR at 300 °C; (d) with PR at 420 °C.

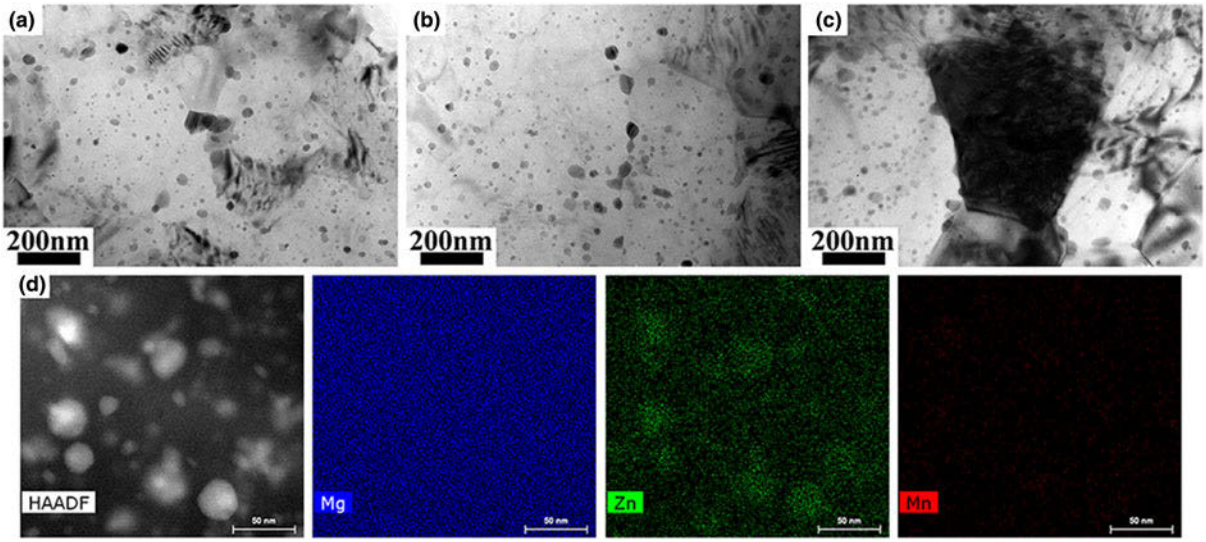


**Figure 4:** TEM bright-field images showing the dynamic precipitation in the as-HSRRed alloy (a) without PR; (b) with PR at 300 °C; (c) with PR at 420 °C and (d) the EDS mapping of the as-HSRRed alloy with PR at 300 °C.

alloy is close to the maximum solid solubility, indicating that the dynamic precipitation can occur easily during the large deformation process such as HSRR. Figure 4 shows the dynamic precipitation in the as-HSRRed alloys with and without PR. A large number of precipitates are observed in the HSRR alloy without PR [Fig. 4(a)]. The smaller precipitates with the short-rod and near-spherical shapes are found within the grains and the other coarser ones with irregular shapes are distributed along grain boundaries. The average size of the irregular precipitates is 47 nm, while those of the short-rod shape and the near-spherical precipitates are 12 and 25 nm, respectively. As shown in Fig. 4(b), the precipitation density in the as-HSRRed alloy with PR at 300 °C increases. It should be noted that the density of the spherical precipitates increases but that of the rod-like precipitates decreases. The average sizes of the spherical and rod-shaped precipitates are 17 and 19 nm, respectively, and that of the irregular precipitates along the grain boundaries slightly decreases to 43 nm. Moreover, the types of the precipitates have no change, but the density of the precipitates decreases and the average size increases with the PR temperature increasing to 420 °C [Fig. 4(c)]. The average size of the irregular precipitates is 47 nm and those of the spherical and the rod-shaped precipitates are 20 and 27 nm, respectively. In general, PR can promote the precipitation but

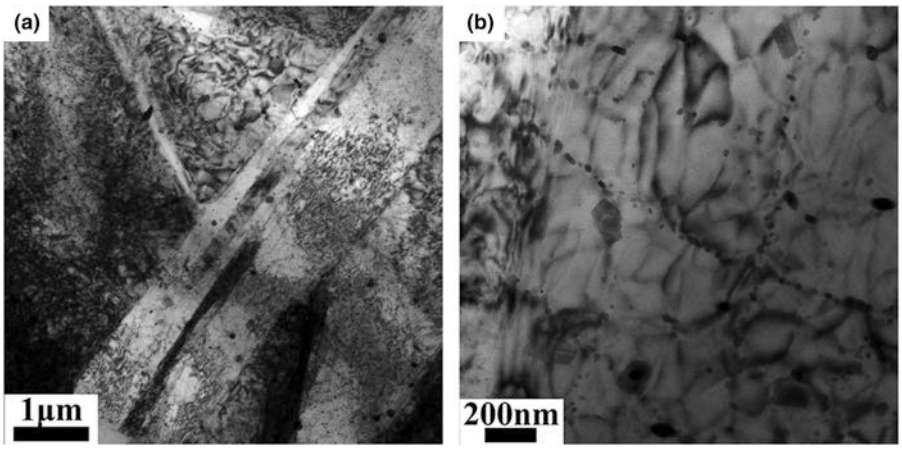


**Figure 5:** TEM bright-field images of the ZM61 alloy after PR at 300 °C with the reduction of 20%.

does not change the types of the precipitates. The average size of the precipitates increases slightly with the higher PR temperature.

Figure 4(d) depicts the elemental mapping images of the as-HSRRed alloy with PR at 300 °C. The precipitates are enriched in the Zn element and no Mn segregation is detected. Our previous study [10] has shown that the precipitates in the pre-rolled alloy are enriched in Zn. That is to see, PR cannot change the types of the dynamic precipitates in HSRR but increases the precipitation density by promoting the nucleation rate. In addition, the pinning effect of the precipitates on the DRX grain boundaries results in the refinement of DRX grains. The refining effect is affected by the density of dynamic precipitates and thus the grain size of the alloy with PR is smaller than that without PR.

To further analyze the influence of PR on the structure of the ZM61 alloy, TEM examination is conducted on the alloy pre-rolled at 300 °C with the reduction of 20%, which is indicated by Fig. 5. A large number of twin lamellae are observed in Fig. 5(a). These twins can separate the original coarse grains into the smaller ones. The twin boundary has a blocking effect on the dislocation movement, resulting in the increment and the entanglement of dislocations and promoting the formation of DRX grains. Clark et al. [16] have found that the twin boundary is the preferential nucleation site for the Mg–Zn phase in the Mg–5Zn alloys and its priority is even higher than the grain boundary. It can be observed in Fig. 5(b) that many fine precipitates are precipitated along the dislocations and some coarse precipitates are also formed in the matrix, indicating that the dynamic precipitates are formed during the PR process. Chen et al. [7] have pointed out that the Mn particles with the long strip shape in the solutionized state would broke into the smaller ones under the deformation force in the subsequent deformation, thus promoting the heterogeneous nucleation of the dynamic precipitates. The crushing effect on Mn particles in the as-HSRRed alloy with PR is better than that in the as-HSRRed alloy without PR, which provides more nucleation sites for the dynamic precipitates. In addition, the precipitates formed in the PR process are retained and thus the precipitation density in the as-HSRRed samples with PR is larger than that without PR.

The influence of PR on DRX during HSRR is mainly achieved by modifying the original structures. A large number of twins are introduced by PR at 300 °C and thus the DRX grains can directly nucleate on the twins, thus accelerating the DRX process. At the same time, the twin boundaries inhibit the movement of dislocations and provide more nucleation sites for DRX grains. Twinning and recrystallization take place after PR at 420 °C with the reduction of 20% and subsequent annealing at 300 °C, and the average grain size before HSRR is about 10 μm. The original DRX grains can be further refined after HSRR by the nucleation at twin boundary to form new DRX grains. However, Jin et al. [17] have pointed out that the local stress concentration in the grains is beyond the reach of the critical shear stress for twinning once the grain size is less than 20 μm. Therefore, it is more difficult for the occurrence of twinning in the alloys pre-rolled at 420 °C during the subsequent HSRR process. PR increases the DRX volume fraction, refines the DRX grains and also promotes the formation of dynamic precipitates, which bring about the enhanced grain refinement strengthening and precipitation strengthening effects and result in the improvement in mechanical properties.

## Interaction between dynamic recrystallization and precipitates

It is clear that DRX can be inhibited by the fine precipitates due to their pinning effect on both high and low angle boundaries [18, 19]. Figure 6 shows the interactions between dynamic precipitates and the other structures, such as dislocations, twins and DRX grains. As shown in Fig. 6(a), the high density of dislocations is observed in the matrix, and some fine precipitates

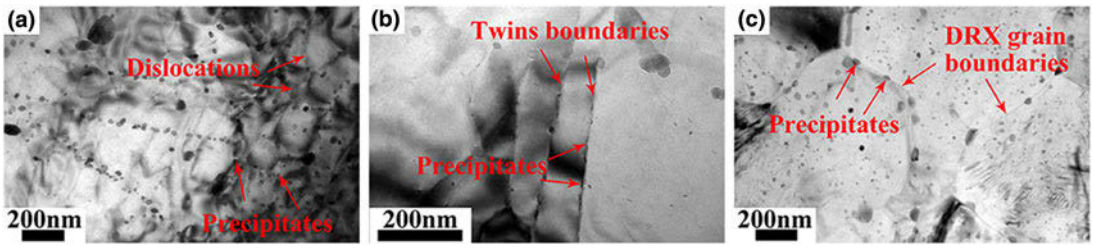


**Figure 6:** TEM bright-field images showing the interactions between dynamic precipitates and dislocations (a), twins (b) and DRX grains (c).

are formed along the dislocations. The high density of dislocations associated with higher energy can promote the precipitation. At the same time, the fine-distributed precipitates can pin dislocations and retard their rearrangement, thus inhibiting the nucleation of continuous DRX. The dense twin lamellae are formed in the alloy [Fig. 6(b)], and the size of the precipitates on the twin boundaries is observed to be larger than that in the internal twins and the matrix. The interactions between twins and the precipitates during deformation are unclear at present. Robsen et al. [20] have found that the increase of the second phase in the Mg–5Zn alloy is helpful to the nucleation of twins during aging. However, Christian et al. [21] have reported that the precipitates in Mg alloy can delay or inhibit the formation of twins, which can be attributed to the complex dislocation structure caused by the precipitates. Many precipitates are also observed in the DRX grain boundaries [Fig. 6(c)], and these precipitates can hinder the movement of DRX grain boundaries and then retard the growth of DRX grains. In summary, the fine precipitates formed in the rolling process can hinder the nucleation and the growth of DRX. However, a large number of twins and dislocations are introduced by PR (Fig. 5) and these twins and dislocations can provide ideal sites for the nucleation of DRX in the subsequent deformation process. The precipitates produced in the PR process can not only promote the precipitation in the subsequent deformation but also retard the growth of DRX grains. As a result, the density of precipitates and the DRX volume fraction increase while the DRX grain size decreases in the as-HSRRed alloy with PR.

## Mechanical properties

Figure 7 shows the mechanical properties of the as-HSRRed alloys with and without PR. The mechanical properties of the as-HSRRed alloy sheets without PR increase firstly and then decrease with the higher temperature. The optimal comprehensive mechanical properties are obtained at 300 °C, with UTS of 369 MPa, YS of 261 MPa and EL of 15.5%. As shown in Fig. 1, the rolling temperature is closely related to the microstructure (DRX volume fraction, DRX grain size, *etc.*) during HSRR. With the HSRR temperature increases from 275 °C to 350 °C, the DRX volume fraction increases from 69 to 82%, and the DRX grain size increases from 1.9 to 3.1 μm. The much lower DRX volume fraction and the poor structural homogeneity are obtained at the lower HSRR temperature, while the higher HSRR temperature will lead to the abnormal grain growth and weaken the fine-grained strengthening effect. Therefore, the as-HSRRed alloy sheet at 300 °C possesses a relatively high DRX volume fraction and a small DRX grain size, resulting in the optimal comprehensive mechanical properties.

The UTS, YS and EL of the sheet subjected to HSRR at 300 °C with PR at 300 °C are 390 MPa, 280 MPa and 14.1%, respectively. As compared with the as-HSRRed alloy sheet without PR, the as-HSRRed alloy sheet with PR at 300 °C has higher UTS and YS values (about 21 and 19 MPa higher, respectively), while shows the lower EL (about 1.4% lower). When the PR temperature increases to 420 °C, the values of UTS and YS are augmented by 12 and 9 MPa, respectively, while the EL value decreases by 0.1% only. The values of UTS and YS decrease but the value of EL increases in the alloy sheets with the higher PR temperature. The different original structures can be ascribed to the different PR temperature, the former of which bring about the differences in DRX and precipitation behaviors during HSRR and lead to the differences in mechanical properties. The main strengthening mechanisms are fine-grained strengthening and precipitation strengthening in the HSRR process. It can be seen from

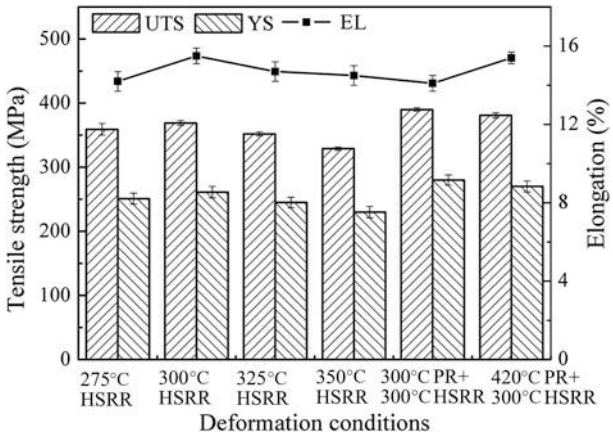


**Figure 7:** Tensile properties of the as-HSRRed ZM61 alloys.

Fig. 2 that the $d_{DRX}$ of the alloy experienced PR at 300 °C is smaller than that experienced PR at 420 °C, resulting in a stronger fine-grained strengthening effect in the alloy experienced PR at 300 °C. In addition, the higher the precipitates density, the stronger the hindering effect on the dislocation movement and the stronger the precipitation strengthening effect. The alloy experienced PR at 300 °C shows a stronger precipitation strengthening effect as its precipitation density is larger than that in the alloy experienced PR at 420 °C (as shown in Fig. 4). Therefore, the alloy experienced PR at 300 °C possesses a higher tensile strength. Similarly, UTS and YS can be improved by the introduction of PR in the as-HSRRed alloy sheets, which is attributed to the stronger fine-grained strengthening and precipitation strengthening resulting from the reduction of $d_{DRX}$ and the increase in the precipitation density.

## Conclusion

The microstructure evolution, DRX and precipitation behaviors of the ZM61 alloy sheets prepared by different PR and HSRR temperatures were studied. The conclusions are as the following.

(i) The $d_{DRX}$ of the as-HSRRed ZM61 alloy prepared at different temperatures (275, 300, 325 and 350 °C) are 1.9, 2.3, 2.6 and 3.1 μm, respectively. The $f_{VDRX}$ are 69, 73, 76 and 82%, respectively. The much lower DRX volume fraction and the poor structural homogeneity are obtained at 275 °C, while the grain growth occurs with the rolling temperature of 350 °C and higher, leading to the reduced fine-grained strengthening effect. The optimal HSRR temperature is 300 °C.

(ii) The $d_{DRX}$ and $f_{VDRX}$ of the alloy sheets prepared by PR at 300 °C with the reduction of 20% followed by HSRR at 300 °C are 1.0 μm and 91%, respectively. The $d_{DRX}$ and $f_{VDRX}$ increase slightly with the higher PR temperature. They are 1.5 μm and 93% with the PR temperature of 420 °C.

(iii) A large number of precipitates can be observed in the as-HSRRed alloy sheets with and without PR. The smaller precipitates with the short-rod and near-spherical shapes are found within the grains and the other coarser ones with the irregular shape are distributed at grain boundaries. PR cannot change the types of precipitates but promote the precipitation. The average size of the precipitates increases slightly with the higher PR temperature. In addition, the pinning effect of the precipitates on the DRX grain boundaries brings about the grain refinement effect.

(iv) The as-HSRRed alloy sheets prepared at 300 °C without PR exhibit the optimal comprehensive mechanical properties, with UTS of 369 MPa, YS of 261 MPa and EL of 15.5%. PR can bring about the improvement of UTS and YS.

## Experimental methodology

The ZM61 (Mg–6Zn–1Mn) alloy ingots were prepared by permanent mold casting. The ingots were subjected to a two-step solution treatment (330 °C for 16 h and 420 °C for 2 h) and then were machined into the plates of 120 mm × 100 mm × 10 mm for HSRR and the plates of 120 mm × 100 mm × 12.5 mm for PR in a twin roll mill with the roller size of Φ360 × 600 mm. The peripheral speed of the roll was 430 mm/s and the twin roll was not heated. Firstly, the HSRR temperature was optimized. The plates (120 mm × 100 mm × 10 mm) were pre-heated at 275, 300, 325 and 350 °C for 6 min, respectively, and then were subjected to HSRR. The rolling temperature was consistent with the pre-heating temperature and the rolling reduction was 80% with the thickness from 10 to 2 mm by a single pass. Secondly, the PR process was optimized. The plates (120 mm × 100 mm × 12.5 mm) were pre-heated at 300 and 420 °C for 10 min, respectively and then pre-rolled with reduction of 20% from 12.5 to 10 mm. The pre-rolled plates were then annealed at 300 °C for 15 min and were subsequently subjected to HSRR in the same twin roll mill with a reduction of 80% from 10 to 2 mm by a single pass at the optimal HSRR temperature. The specific rolling process and the rolling parameters can be found in the literature [11, 22].

The as-rolled microstructures were examined on the sections perpendicular to the transverse direction (TD) and the rolling direction (RD). The picric acid solution (0.8 g picric acid + 2 mL acetic acid + 3 mL water + 20 mL alcohol) was used as the etching agent for the metallographic analysis and the etching time was about 10 s. The microstructure was observed on LeitzMM-6 optical microscope (OM). The DRX grain size ($d_{DRX}$) and the volume fraction ($f_{VDRX}$) were statistically analyzed by the line intercept method and the Image Pro Plus software, respectively. About 30 fields of view and 7 typical images were adopted for each sample. The $f_{VDRX}$ was calculated as the following. Firstly, the total pixel points ($A$) of an image and the pixel points ($a$) of the deformation area in the image were obtained by the Image-Pro Plus 6.0 software. Secondly, the $f_{VDRX}$ of the alloy was calculated by $f_{VDRX} = (A - a)/A$. Finally, the $f_{VDRX}$ of each sample was the average value of seven different images. The characteristics of the precipitates in the alloys after HSRR with or without PR treatment were analyzed by Titan G2 60-300 transmission electron microscopy (TEM). The mechanical properties were measured on Instron

3369 electronic universal testing machine. The tensile specimens were cut from the as-rolled sheets along RD with 15 mm in gauge length and 4 mm × 2 mm in cross section. The tensile direction was parallel to RD and the tensile testing was conducted with the initial strain rate of $5.6 \times 10^{-4}$ $s^{-1}$ at room temperature.

## Acknowledgments

The authors are grateful to the support of the National Natural Science Foundation of China (51471066, 51571089) and Natural Science Foundation of Hunan Province, China (2019JJ40044).

## Data availability

The raw/processed data required to reproduce these findings cannot be shared at this time as the data also form part of an ongoing study.

## Declaration of competing interest

None.

## References

1. **A.-A. Luo**: Magnesium casting technology for structural applications. *J. Magnesium Alloys* **1**, 2–22 (2013).
2. **A.-A. Luo**: Materials comparison and potential applications of magnesium in automobiles. In *Essential Readings in Magnesium Technology*, H.-I. Kaplan, J.-N. Hryn and B.-B. Clow eds. (Springer International Publishing, Berlin, 2016); pp. 25–34.
3. **T. Mukai, M. Yamanoi, H. Watanabe, and K. Higashi**: Ductility enhancement in AZ31 magnesium alloy by controlling its grain structure. *Scr. Mater.* **45**(1), 89–94 (2001).
4. **J.-F. Nie**: Precipitation and hardening in magnesium alloys. *Metall. Mater. Trans. A* **43**(11), 3891–3939 (2012).
5. **W.-M. Mao and X.-B. Zhao**: *The recrystallization and grain growth of the metals* (Metallurgical Industry Press, Beijing, 1994), pp. 201–209.
6. **J. Peng, X.-S. Tong, B.-J. Lv, Y. Pen, and F.-S. Pan**: Hot compression deformation behaviour and dynamic recrystallization of Mg-6Zn-1Mn magnesium alloy. *Trans. Mater. Heat. Treat.* **34**(5), 180–185 (2013).
7. **C. Chen, J.-H. Chen, H.-G. Yan, B. Su, M. Song, and S.-Q. Zhu**: Dynamic precipitation, microstructure and mechanical properties of Mg-5Zn-1Mn alloy sheets prepared by high strain-rate rolling. *Mater. Des.* **100**, 58–66 (2016).
8. **S.-Q. Zhu, H.-G. Yan, J.-H. Chen, Y.-Z. Wu, J.-Z. Liu, and J. Tian**: Effect of twinning and dynamic recrystallization on the high strain rate rolling process. *Scr. Mater.* **63**(10), 985–988 (2010).
9. **B. Song, N. Guo, T.-T. Liu, and Q.-S. Yang**: Improvement of formability and mechanical properties of magnesium alloys via pre-twinning: A review. *Mater. Des.* **62**, 352–360 (2014).
10. **J.-M. Jiang, J. Wu, S. Ni, H.-G. Yan, and M. Song**: Improving the mechanical properties of a ZM61 magnesium alloy by pre-rolling and high strain rate rolling. *Mater. Sci. Eng., A* **712**, 478–484 (2018).
11. **J. Wu, J.-H. Chen, H.-G. Yan, W.-J. Xia, B. Su, L. Yu, G.-S. Liu, and M. Song**: Enhancing the mechanical properties of high strain rate rolled Mg-6Zn-1Mn alloy by pre-rolling. *J. Mater. Sci.* **52**(17), 10557–10566 (2017).
12. **B. Song, R.-L. Xin, G. Chen, X.-Y. Zhang, and Q. Liu**: Improving tensile and compressive properties of magnesium alloy plates by pre-cold rolling. *Scr. Mater.* **66**(12), 1061–1064 (2012).
13. **S.-G. Hong, S.-H. Park, and S.-L. Chong**: Role of {10-12} twinning characteristics in the deformation behavior of a polycrystalline magnesium alloy. *Acta Mater.* **58**(18), 5873–5885 (2010).
14. **S.-H. Park, H.-S. Kim, J.-H. Bae, C.-D. Yim, and B.-S. You**: Improving the mechanical properties of extruded Mg-3Al-1Zn alloy by cold pre-forging. *Scr. Mater.* **69**(3), 250–253 (2013).
15. **J.-B. Clark, L. Zabdyr, Z. Moser, and A.-H. Nayeb**: *Phase Diagrams of Binary Magnesium Alloys* (ASM International, Metals Park, OH, 1988), p. 353.
16. **J.-B. Clark**: Transmission electron microscopy study of age hardening in a Mg-5 wt.% Zn alloy. *Acta Metallurgy* **13**(12), 1281–1289 (1965).
17. **L. Jin, J. Dong, R. Wang, and L.M. Peng**: Effects of hot rolling processing on microstructures and mechanical properties of Mg-3%Al-1%Zn alloy sheet. *Mater. Sci. Eng., A* **527**(7–8), 1970–1974 (2010).
18. **M. Hradilová, F. Montheillet, A. Fraczkiewicz, C. Desrayaud, and P. Lejček**: Effect of Ca-addition on dynamic recrystallization of Mg-Zn alloy during hot deformation. *Mater. Sci. Eng., A* **580**, 217–226 (2013).
19. **F.-J. Humphreys and M. Hatherly** : *Recrystallization and Related Annealing Phenomena*, 2nd ed. (Elsevier, Oxford, 2004), pp. 208–305.
20. **J.-D. Robson, N. Stanford, and M.-R. Barnett**: Effect of particles in promoting twin nucleation in a Mg-5Zn alloy. *Scr. Mater.* **63**(8), 823–826 (2010).
21. **J.-W. Christian and T.-C. Wang**: Deformation twinning and its effect on crack extension. *Acta Mater.* **46**(15), 5313–5321 (1998).
22. **S.-Q. Zhu, H.-G. Yan, J.-H. Chen, Y.-Z. Wu, B. Su, Y.-G. Du, and X.-Z. Liao**: Feasibility of high strain-rate rolling of a magnesium alloy across a wide temperature range. *Scr. Mater.* **67**(4), 404–407 (2012).